Applications of ANNs in the Field of the HCPV Technology

Florencia Almonacid, Adel Mellit and Soteris A. Kalogirou

Abstract High-concentrator photovoltaic (HCPV) devices are based on the use of multijunctions solar cells and optical devices. Therefore, the electrical modelling of an HCPV device presents a great level of complexity. Several artificial neural network (ANN)—based models have been developed to try to address this issue. In this chapter, a review of the developed ANN—based models developed to try to address some issues related with the field of high concentrator PV technology is reported. In addition, the results obtained from the application of some of these models to estimate the electrical parameters of an HCPV module—such as maximum power, short-circuit current, and open-circuit voltage—are presented. The results show that the ANNs are a useful tool for modelling HCPV applications.

1 Introduction

High-concentrator photovoltaic (HCPV) technology is based on the use of optical devices that focus the light received from the Sun on the solar cell surface. The aim of these systems is to decrease the cost of the electricity by decreasing the semiconductor material by mounting less expensive optical devices [1]. HCPV technology is widely based on the use of high efficiency multijunction (MJ) solar cells; a primary optical element (usually a Fresnel lens), which concentrates the light; and a secondary optical element, which receives the light from the primary one to

F. Almonacid (✉)
IDEA Research Group, University of Jaén, Campus Lagunillas, 23071 Jaén, Spain
e-mail: facruz@ujaen.es

A. Mellit
Faculty of Sciences and Technology, Renewable Energy Laboratory, Jijel University, 18000 Jijel, Algeria

S.A. Kalogirou
Department of Mechanical Engineering and Materials Sciences and Engineering, Cyprus University of Technology, P.O. Box 50329, 3603 Limassol, Cyprus

P. Pérez-Higueras and E.F. Fernández (eds.), *High Concentrator Photovoltaics*, Green Energy and Technology, DOI 10.1007/978-3-319-15039-0_12

homogenize light and improve the angular acceptance angle [2]. An HCPV module is made up of MJ solar cells, an optical system for each cell, and the rest of the components required to generate electricity and dissipate the heat produced on the solar cell surface. MJ solar cells and HCPV modules have already reached high efficiencies, which are expected to continue growing in the next few years [3–5]. Thus, HCPV could play an important role in the energy generation market in the coming years [6]. However, due to the use of MJ solar cells and optical elements, the electrical modelling of HCPV devices shows a significant level of complexity than for conventional photovoltaic (PV) technology.

Artificial neural networks (ANNs) have proven to be helpful in solving complex problems and studying nonlinear systems. In the field of PVs, ANNs have been successfully applied to solve different issues [7–9]. For instance, ANNs have been used to:

- estimate and predict solar radiation data [10–14],
- estimate the maximum power (P_m) and normal operating power of a flat PV module [15, 16],
- size, model, and simulate both stand-alone PV systems [17, 18] and PV systems with a maximum power-point tracking controller [19, 20],
- predict the equivalent circuits parameters of a flat PV module [21],
- select a suitable model for characterising PV devices [22],
- obtain the current–voltage (I–V) curves of different flat-plane panels [23, 24],
- or to estimate the energy production of grid-connected PV systems [25, 26].

Due to the advantages of the ANNs to solve complex and nonlinear problems related with the field of PVs and the great level of complexity of electrical modelling of HCPV devices, in the recent years several authors have applied different ANNs to solve various problems related with this new technology. In this chapter, a review of the ANNs developed to address various issues related with the HCPV is presented, and examples of the application of ANNs in this field are given. In particular, the results obtained in the application of some of these ANNs to estimate the main electrical parameters of an HCPV module—including P_m, short-circuit current (I_{sc}), and open-circuit voltage (V_{oc})—are presented.

2 Application of ANNs to Estimate of Direct Solar Irradiation

Due to the use of lenses that concentrate light on the solar cell, the HCPV devices operate only with direct normal irradiance (DNI). So the DNI is especially important for the characterization, management, and operation of HCPV modules, systems, and power plants. DNI is affected by phenomena that are difficult to forecast such as cirrus clouds, wildfires, dust storms, and episodic air pollution events, which can decrease DNI by ≤30 % on otherwise cloud-free days [27].

Because of this, the modelling and prediction of the DNI is a difficult task, and several authors have used ANN-based models to address this issue. A complete review about the solar data forecast by using artificial intelligence methods including DNI and neural network can be found in [28].

A Bayesian neural network was developed to model direct solar irradiance by Lopez et al. [29]. A relevance-determination method was also employed to obtain the relative relevance of a large set of meteorological and radiometric variables. Results show that the more relevant parameters are the clearness index (K_t) and air mass (AM).

In [30], the authors developed an ANN model to estimate beam solar radiation. A new parameter known as the "reference clearness index" was introduced, which is defined as the ratio of the measured beam solar radiation at normal incidence to the beam solar radiation as computed by Hottel's clear-day model. Results show that root mean square error (RMSE) in the ANN model varies 1.65–2.79 % for Indian regions.

Mishra et al. [31] developed a self-consistent model for the estimation of direct solar radiation in the Indian zone. An ANN-based model was used for the estimation of the K_t. The model predictions for the Indian region were found to be in good agreement with the measurements.

An adaptive model for predicting hourly global, diffuse, and direct solar irradiance was developed in [32]. A comparison between a Feed-Forward Neural Network (FFNN) and the proposed adaptive model was also presented. It was shown that the FFNN was able to predict the DNI with acceptable accuracy at Jeddah, King of Saudi Arabia (KSA). They observed that ANN performed better than the designed adaptive alpha-model with a correlation coefficient of 98 %.

In [33], the author developed an ANN model for estimating of monthly average daily direct solar radiation. According to the author, a correlation coefficient of 0.998 was obtained with mean bias error (MBE) of 0.005 MJ/m^2 and an RSME of 0.197 MJ/m^2.

In [34], the authors developed forecasting models for hourly solar irradiation using ANNs for lead times of ≤6 days. Model inputs included current and forecasted meteorological data obtained from the United States National Weather Service's forecasting database and solar geotemporal variables. The gamma test was combined with a genetic algorithm to select the more relevant inputs. According to the authors, the estimation of DNI is much more difficult to predict reliably; the RMSE values obtained on same-day forecasts are in the range of 28–35 %.

Several ANNs were developed by Rodrigo et al. [35] for the generation of DNI hourly time series for some Spanish locations. In particular, different architectures of multiple linear perceptron (MLP) neural networks were used with three different configurations. The designed model could be used for the estimation of the energy that will be produced by concentrating PV systems, to perform economic analysis, and to supervise plant operation. The developed models were tested in different locations. The RMSE among real data and synthetic data for the three configurations and for the different locations considered are in the range 0.01–0.27. Results show that the ANNs yield better results for locations in the south of Spain.

Rehman and Mohandes [36] used a radial basis function (RBF) network for modelling the diffuse and direct normal solar radiation for sites in KSA based on

Table 1 Summary of the applications of ANNs for predicting the DNI

#	Authors	Ref.	Year	ANN
1	Mellit	[28]	2008	Feed-forward neural network, radial basis function neural network, and neural networks
2	Lopez et al.	[29]	2005	Bayesian neural network with Automatic Relevance Determination (ARD)
3	Alam et al.	[30]	2006	Feed-forward back-propagation neural network
4	Mishra et al.	[31]	2008	Feed-forward back-propagation neural network
5	Mellit et al.	[32]	2010	Feed-forward back-propagation neural network
6	Mubiru	[33]	2011	Feed-forward back-propagation neural network
7	Marquez and Coimbra	[34]	2011	Feed-forward back-propagation neural network
8	Rodrigo et al.	[35]	2012	Feed-forward back-propagation neural network
9	Rehman and Mohandes	[36]	2012	Radial basis function neural networks
10	Marpu et al.	[37]	2013	Feed-forward back-propagation neural network
11	Chu et al.	[38]	2013	Feed-forward neural network with genetic algorithm

input data such as day number, global solar radiation, ambient temperature, and relative humidity. The results indicate that the RBF (with 50 hidden neurons and 0.1 spread constant) predicts direct normal solar radiation with mean absolute percentage error of 0.016 and 0.41 for diffuse solar radiation.

A regionally based ANN model to retrieve the DNI at the surface of the United Arab Emirates (UAE) was developed by Marpu et al. [37]. The results are promising when estimating the solar irradiance at a 15-minute temporal resolution and a 3-km spatial resolution. The inputs of the designed model were six SEVIRI (on-board Meteosat Second Generation satellite) thermal channels along with several time- and season-dependent parameters, namely the solar zenith angle, solar time, day number, and eccentricity correction.

Recently, Chu et al. [38] designed a novel smart forecasting model for intra-hour DNI. The authors combined sky image processing with ANN optimization schemes. The hybrid forecast models achieved statistically robust forecasting skills in excess of 20 % over persistence both for forecasts 5 and 10 min ahead, respectively. Table 1 lists the applications of ANNs for modelling and prediction of DNI and lists the type of ANN employed in each case.

3 Application of ANNs for the Electrical Modelling of HCPV Devices

As in any kind of energy system, modelling the electrical output of a PV device is crucial for the system design and energy prediction. However, the electrical modelling of HCPV modules and systems shows a significantly greater level of

complexity than conventional PV technology. Due to the use of MJ solar cells and optical devices, HCPV modules and systems show a strong spectral dependence. To quantify the spectral changes and to evaluate how these affect the behaviour of an HCPV device is not a trivial issue [39, 40]. In addition, as in conventional PV technology, the cell temperature (T_c) is an important input in models used for the electrical characterization of HCPV devices because the temperature at which cells are working in an HCPV module affects its performance. However, one of the problems in HCPV technology is that the direct measurement of this temperature is a complex task because it requires access inside the module [41].

Because of this difficulty, in recent years the scientific community has devoted efforts in developing ANN-based models which try to solve some of these issues.

3.1 Application of ANNs to Modelling Multi-junction Solar Cells

The PV solar cells used in HCPV technology are made of several p-n junctions (usually three junctions) of III–V semiconductor materials of the periodic table. Each p-n junction has a different band gap and is interconnected in series with the others to optimize the absorption of the solar spectrum and increase the efficiency of the solar cell electricity conversion [42]. Thus, although single-junction (SJ) solar cells are mainly influenced by changes in irradiance and temperature, MJ solar cells show complex behaviour because their performance is also strongly influenced by changes in solar spectrum. Due to this, Patra et al. [43–46] proposed approaches based on ANN to characterize these devices.

In [43] and [44], an ANN based-model was proposed to characterize dual-junction (DJ) GaInP/GaAs solar cells. The authors used four multilayer perceptrons: one for estimating the tunnelling effects of a solar cell and the other three for estimating the external quantum efficiency (EQE) and the I–V characteristic, both under 1 sun and in dark, for the DJ solar cell. The inputs for ANNs are the voltage for estimating the tunnelling effects and the I–V characteristic as well as the irradiation wavelength (λ) for estimating the EQE. The results were compared with experimental and simulated data through Silvaco ATLAS software [47]. The results showed that compared with the results obtained through ATLAS, the MLP-based model was able to predict DJ solar cell parameters more closely to that of experimental ones.

In [45], a novel Chebyshev neural network-based model for a DJ GaInP/GaAs solar cell was developed to predict the EQE and the I–V characteristics, both at one sun and dark levels. The inputs of the model are the same as those in the previous case.

In [46], an ANN-based model was used to estimate the EQE and the performance of triple-junction InGaP/GaAs/Ge solar cells under the influence of a wide range of charged particles. The inputs of the models are the wavelength (λ), the proton energy (η), and the fluence (f). The results show that the ANN-based models

perform quite well in the estimation of EQE of the solar cell under the influence of proton energy ranging from 30 keV to 10 MeV with fluence levels ranging from 10^{10} to 10^{14} ion/cm^2.

3.2 Application of ANNs to Modelling HCPV Modules

3.2.1 Application of ANNs to Estimate the Maximum Power of a HCPV Module

Due to the use of MJ solar cells and lenses, HCPV modules are mainly influenced by changes in irradiance, spectrum, temperature, and wind speed (W_s). Taking this into account, the output of HCPV modules could be expressed as a function of these parameters:

$$P_m = f(B, S, T, W_s) \tag{1}$$

The relation between these parameters and the output of an HCPV module is complex and nonlinear, so the use of ANN-based models has been proposed by several authors to try to find this relation.

Almonacid et al. [48] developed an ANN-based model, in particular an MLP, to find the relation between the output of an HCPV and the main parameters that affected its performance. The input parameters used by the model are as follows:

- the DNI to evaluate how the changes in the irradiance affect the performance of an HCPV module
- AM and precipitable water (PW) to evaluate the spectrum because these are, together with clouds and aerosol optical depth (AOD), the parameters with the largest impact on spectral changes [49, 50] and are also easy to obtain from the data provided by a meteorological station [51–54]
- air temperature (T_{air}) to evaluate the temperature of the HCPV module; and
- the wind speed (W_s).

Coefficients of neural networks are obtained from outdoor monitored data. The results show that the ANN based-model could be used to estimate successfully the output of an HCPV module with a MBE of 0.07 %, an RMSE of 2.91 %, and an R^2 of 0.99.

This approach has also been followed by Rivera et al. [55]. In this case, a cooperative competitive hybrid algorithm for RBF networks was implemented. This model uses as input the average photon energy [56, 57] to quantify the spectral influences on the P_m of an HCPV module. This is a single value in eV that characterizes the shape of the spectrum. A spectroradiometer is required for obtaining this input. The rest of the inputs of the model are DNI to evaluate how the changes in the irradiance affect the performance of an HCPV module, T_{air} to evaluate the temperature, and W_s. The coefficients of the neural network are obtained from outdoor monitored data. The model obtained gives an error of approximately 3.3 %.

3.3 Application of ANNs to Estimate the Electrical Characteristics of an HCPV Module

As already indicated, the output of an HCPV module is significantly affected by changes in irradiance, spectrum, and temperature. A different approach for electrical modelling of these devices is based on the premise that the electrical parameters of an HCPV module can be estimated by applying models and equations used for conventional PV technology from the DNI, corrected spectrally, and the T_c [58, 59]. According to this approach, two ANNs for estimating these parameters have been proposed in [41, 60].

Application of ANNs to estimate the spectrally corrected direct normal irradiance

The spectrally corrected DNI (DNI_c) is defined as the portion of the incident spectrum that an HCPV module is able to convert into electricity expressed here as:

$$\mathrm{DNI}_c = \frac{\min\left(\int E_b(\lambda)\eta(\lambda)SR_i(\lambda)\mathrm{d}\lambda\right)}{\min\left(\int E_{b,\mathrm{ref}}(\lambda)\eta(\lambda)SR_i(\lambda)\mathrm{d}\lambda\right)} \int E_{b,\mathrm{ref}}(\lambda)\mathrm{d}\lambda \tag{2}$$

where the index i represents the junction considered, λ is the wavelength, $SR_i(\lambda)$ is the spectral response of the i-junction, $E_b(\lambda)$ is the spectral distribution of the DNI, and $\eta(\lambda)$ is the optical efficiency of the HCPV module.

The advantage of this approach is that the spectral effects of an HCPV device are quantified by adjusting only the incident DNI [58].

Taking this into account, an ANN-based model for DNI_c was presented in [60]. The inputs of the model are the main meteorological parameters that influence the spectral distribution of the DNI and the performance of an HCPV module: AM, AOD, and PW. Results show that the method is able to predict spectrally corrected normal irradiance with an RMSE of 2.92 %, an MBE of −0.12 %, and a R^2 of 0.98.

Application of ANNs to estimate the cell temperature of a HCPV module

The operating temperature of the solar cell is a crucial issue to characterize the electrical behaviour of a PV device. However, the measurement of this temperature in an HCPV module is a complex task due to its special features that do not allow one to access the cell. To solve this problem, several authors have attempted different approaches [41, 61]. One of these is based on the premise that the T_c can be obtained from the main meteorological parameters that have an influence in this temperature: DNI, T_{air}, and W_s. Using a linear expression [62]:

$$T_c = T_{\mathrm{air}} + a\mathrm{DNI} + bW_s \tag{3}$$

where a and b are empirical parameters obtained from outdoor monitored data.

Table 2 Summary of applications of artificial neural networks for modelling HCPV devices

No.	Authors	Ref.	Year	ANNs
ANN for modelling MJ solar cells				
1	Patra and Maskell, Patra	[43, 44]	2010 2011	Feed-forward back-propagation neural network
2	Patra	[45]	2011	Chebyshev neural network
3	Patra and Maskell	[46]	2012	Feed-forward back-propagation neural network
ANNs for modelling HCPV modules				
4	Almonacid et al.	[48]	2014	Feed-forward back-propagation neural network
5	Rivera et al.	[55]	2013	Radial basis function network with a cooperative-competitive hybrid algorithm
6	Fernández et al.	[41]	2014	Feed-forward back-propagation neural network
7	Fernández and Almonacid	[60]	2014	Feed-forward back-propagation neural network

According to this approach, an ANN-based model was presented in [41]. This model attempts to characterise the relationship between the T_c and the main meteorological parameters that affect it. The input parameters are DNI, T_{air}, and W_s. Results show that the ANN-based model significantly improves the results of the method based on a linear expression with an R^2 of 0.95, a relative RMSE of 4.80 %, and an absolute RMSE of 3.24 °C. Table 2 lists the applications of ANNs for modelling HCPV devices and also indicates the type of ANN employed in each case.

4 Examples of Applications

In this section, some examples of the applications of the ANNs for the characterization of HCPV modules are presented. The first example concerns the P_m of an HCPV estimated using the ANN developed by Almonacid et al. in [48]. In the second part, the V_{oc} and the I_{sc} of an HCPV module will be calculated from the DNI_c and the T_c according to the approach presented in [58, 59]. The ANNs developed in [41, 60] have been used to estimate the spectrally corrected normal irradiance and the T_c for an HCPV module.

4.1 Experimental Campaign

To conduct this study, an HCPV module was measured for 6 months in the Centro de Estudios Avanzados en Energía y Medio Ambiente at the University of Jaén. The module is made up of 20 lattice-matched MJ solar cells connected in series (N_s)

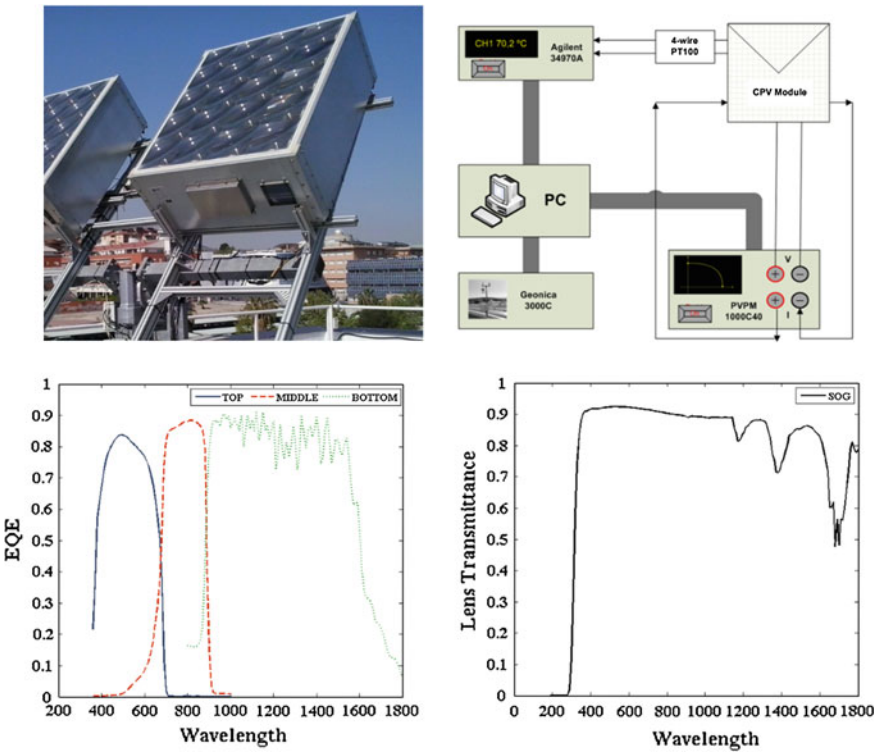

Fig. 1 *Top left* Photograph of the HCPV module considered in the study. *Top right* Scheme of the experimental set-up to measure the electrical parameters of the HCPV module and the main parameters necessary to train the ANN. *Bottom left* EQE of the MJ solar cells of the HCPV module. *Bottom right* Transmittance of the Fresnel lenses used in the HCPV module considered

with a silicon-on-glass Fresnel lens on each cell (Fig. 1, top left). Figure 1 shows the EQE of the MJ solar cells and the transmittance of the lens of the HCPV module used in this study. Table 3 shows the main electrical parameter of the HCPV module.

The experimental set-up (Fig. 1, top right) used to measure the electrical characteristic of the HCPV module and the main parameters necessary to train the ANNs for estimating P_m, DNI_c and the T_c, is made up of the following:

Table 3 Electrical characteristics of the module under study measured at outdoor reference conditions: DNI = 900 W/m^2, T_{air} = 20 °C, and AM = 1.5, for wind speed lower than 1 m/s

Electrical parameters of the HCPV module	
Maximum power (P_m)	232 W
Open circuit voltage (V_{oc})	57.6 V
Short circuit current (I_{sc})	5.3 A

Table 4 Maximum, minimum, and average values of the parameters used as inputs of the ANNs for estimating P_m, DNI_c, and T_c

Parameter	Maximum	Minimum	Average
DNI (W/m^2)	978.42	235.27	763.00
T_{air} (°C)	40.36	3.74	26.12
W_s (m/s)	9.76	0.00	1.34
AM	9.05	1.02	1.92
AOD	0.55	0.04	0.19
PW (cm)	3.29	0.39	1.71

- a high-accuracy two-axis solar tracker to keep the HCPV module always pointing toward the solar rays so lenses are able to focus the radiation on the small solar cell area;
- a four-wire electronic load to measure the electrical parameters of the module;
- a four-wire PT100 placed close to the solar cell to measure the T_c; and
- a meteorological station placed at the roof of the centre to record the main atmospheric parameters such as DNI, T_{air}, W_s, or humidity.
- the values of AOD and PW, which were not provided by the meteorological station, were obtained from MODIS Daily Level-3 data source [63].

Table 4 shows the maximum, minimum, and average values of the parameters used as inputs of the different ANNs used in the study.

4.2 Estimation of the Maximum Power of a HCPV Module

The ANN developed in [48] has been applied to estimate the P_m of the HCPV module. The inputs of the ANN-based model are DNI, AM, PW, T_{air}, and W_s. The structure of the ANN consists of tree layers: the input layer, which has five nodes; the hidden layer, which has seven nodes; and the output layer, which has one node that corresponds to the P_m of the HCPV module. This architecture was trained with the Levenberg–Marquardt back-propagation algorithm to determine the coefficients of the ANN. To train and test the ANN, a set of outdoor measurements, including the output of the HCPV module and the meteorological parameters, were used for a wide range of operating conditions (Table 4). Table 5 shows the coefficient of multiple determination (R^2), the RMSE, the mean absolute error (MAE), and the MBE between actual data and data predicted by the ANN-based model.

Figure 2 shows an example in the estimation of the P_m of the HCPV module using the ANN based-model for two different days (summer and winter days).

Table 5 Values of the parameters R^2, RMSE, MAE, and MBE between actual data and predicted data by the ANN-based model for estimating the maximum power of the HCPV module considered

R^2	RMSE (%)	MAE (W)	MBE (%)
0.98	2.78	4.09	−0.01

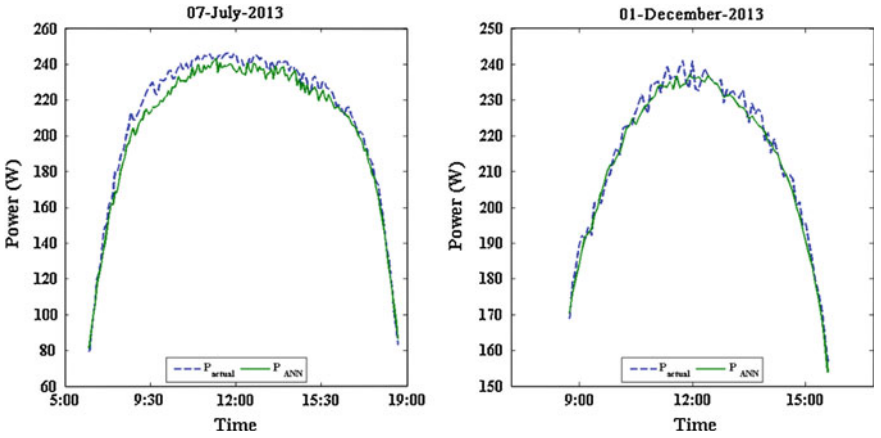

Fig. 2 *Left* Actual maximum power of the HCPV module considered versus predicted maximum power by the ANN-based model for a summer day (07 July 2013). *Right* Actual maximum power of the HCPV module considered versus predicted maximum power by the ANN-based model for a winter day (01 December 2013)

Table 6 Maximum, minimum, and average values of the parameters used as inputs for the two examples days (summer and winter day)

	Summer day (07/07/2013)			Winter day (01/12/2013)		
Parameter	Maximum	Minimum	Average	Maximum	Minimum	Average
DNI (W/m^2)	924.87	378.46	797.77	931.97	674.10	863.94
T_{air} (°C)	36.8	27.8	33.24	13.12	4.72	9.44
W_s (m/s)	6.70	0.25	3.93	3.91	0	1.25
AM	6.42	1.00	1.82	4.30	1.87	2.42
AOD	0.15	0.15	0.15	0.09	0.09	0.09
PW (cm)	1.82	1.82	1.82	0.78	0.78	0.78

Table 6 shows the maximum, minimum, and average values of the parameters used as input of the ANN for the two example days.

4.3 Estimation of the Electrical Parameters of a HCPV Module

According to the approach that the electrical performance of an HCPV device can be quantified from the DNI_c and T_c [58, 59], the V_{oc}, and the I_{sc} of the HCPV module considered can be estimated from equations used in conventional PVs:

$$I_{sc} = \frac{I_{sc}^*}{G^*} G\left(1 + \gamma\left(T_c^* - T_c\right)\right) \tag{4}$$

$$V_{oc} = V_{oc}^*\left(1 + \beta\left(T_c^* - T_c\right)\right) + N_s \frac{mkT_c}{q} \ln\left(\frac{G}{G^*}\right) \tag{5}$$

where I_{sc}^*, G^*, T_c^*, and V_{oc}^* are the I_{sc}, solar global irradiance, T_c, and V_{oc} at reference conditions; γ and β are the T_c coefficient of the I_{sc} and the V_{oc}, respectively; m is the effective ideality factor of the cell; k is the Boltzmann constant; and q is the electron charge.

Equations (4) and (5) must be adapted to HCPV as follows:

$$I_{sc} = \frac{I_{sc}^*}{\mathrm{DNI}^*} \mathrm{DNI}_c\left(1 + \gamma\left(T_c^* - T_c\right)\right) \tag{6}$$

$$V_{oc} = V_{oc}^*\left(1 + \beta\left(T_c^* - T_c\right)\right) + N_s \frac{mkT_c}{q} \ln\left(\frac{\mathrm{DNI}_c}{\mathrm{DNI}^*}\right) \tag{7}$$

where DNI^* is the DNI at reference conditions and DNI_c is the spectrally corrected DNI. The various parameters for the module considered are $m = 3$, $\gamma = 0.002\ ^\circ\mathrm{C}^{-1}$ and $\beta = 0.0015\ ^\circ\mathrm{C}^{-1}$ for the HCPV.

4.4 Estimation of the Spectrally Corrected Direct Normal Irradiance

To estimate the DNI_c of the HCPV module considered, the ANN developed in [60] was applied. The inputs of the ANN are AM, AOD, and PW, and the ANN has five nodes in the hidden layer and one node in the output layer corresponding to the spectral correction function. This architecture was trained with the Levenberg–Marquardt back-propagation algorithm to determine the coefficients of the ANN. To train and test the ANN, a set of outdoor measurements were used for a wide range of operating conditions listed in Table 4. Table 7 lists the R^2, the RMSE, the MAE, and the MBE—all of which are considered very adequate—between actual and predicted data using the ANN-based model.

Figure 3 shows an example of the DNI measured during 2 days (summer and winter) versus the DNI_c predicted by the ANN based-model for the HCPV module.

Table 7 Values of the parameters R^2, RMSE, MAE, and MBE between actual data and predicted data by the ANN-based model for estimating the spectrally corrected direct normal irradiance

R^2	RMSE (%)	MAE (W/m^2)	MBE (%)
0.98	3.19	17.50	−0.16

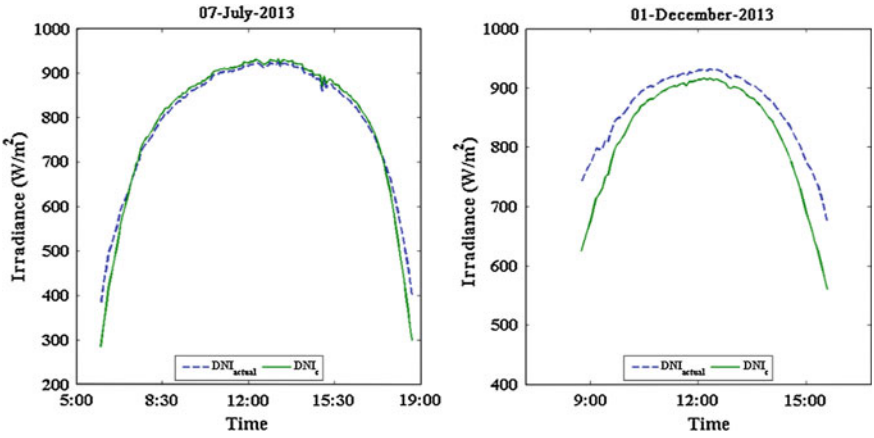

Fig. 3 *Left* Actual direct normal irradiance versus spectrally corrected direct normal irradiance predicted by the ANN-based model for a summer day (07 July 2013). *Right* Actual direct normal irradiance versus spectrally corrected direct normal irradiance predicted by the ANN-based model for a winter day (01 December 2013)

Table 6 shows the maximum, minimum, and average values of the parameters used as input to the ANN for the 2 example days.

As can be seen from Fig. 3, although the maximum level of DNI reached on winter and summer is similar (approximately 900 W/m^2), the DNI$_c$ is lower in winter. This could be mainly explained because the AM values are significantly greater in the winter than in summer, so the portion of the incident spectrum that an HCPV module is able to convert into electricity is lower due to spectral losses. This also can be observed at the sunrise and sunset (both in winter and summer) when the AM values are greater and the DNI$_c$ is lower than DNI.

4.5 Estimation of the Cell Temperature

To estimate the T_c of the HCPV module considered, the ANN developed in [41] has been used. The inputs of the ANN are: T_{air}, DNI and W_s, and the ANN has five nodes in the hidden layer and one node in the output layer corresponding to the T_c of the HCPV module. This architecture was trained with the Levenberg–Marquardt back-propagation algorithm, to determine the coefficients of the ANN. To train and test the ANN, a set of outdoor measurements including the T_c of the HCPV module and the meteorological parameters were used for a wide range of operating conditions, listed in Table 4. Table 8 shows the R^2, RMSE, MAE and the MBE between actual data and predicted data using the ANN-based model.

Table 8 Values of the parameters R^2, RMSE, MAE, and MBE between actual data and predicted data by the ANN-based model for estimating the cell temperature of the HCPV module considered

R^2	RMSE (%)	MAE (°C)	MBE (%)
0.90	5.16	2.51	0.00

Figure 4 shows an example of the T_c of the HCPV module measured during 2 days (summer and winter day) versus the T_c predicted by the ANN based-model. Table 6 shows the maximum, minimum, and averages values of the parameters used as input of ANN for the two example days.

4.5.1 Estimation of the Short-Circuit Current and the Open-Circuit Voltage

Once the values of the DNI_c and T_c are available, it is possible to estimate the I_{sc} and the V_{oc} using Eqs. (6) and (7). Table 9 shows the R^2, RMSE, MAE, and MBE between actual and predicted data using Eqs. (6) and (7).

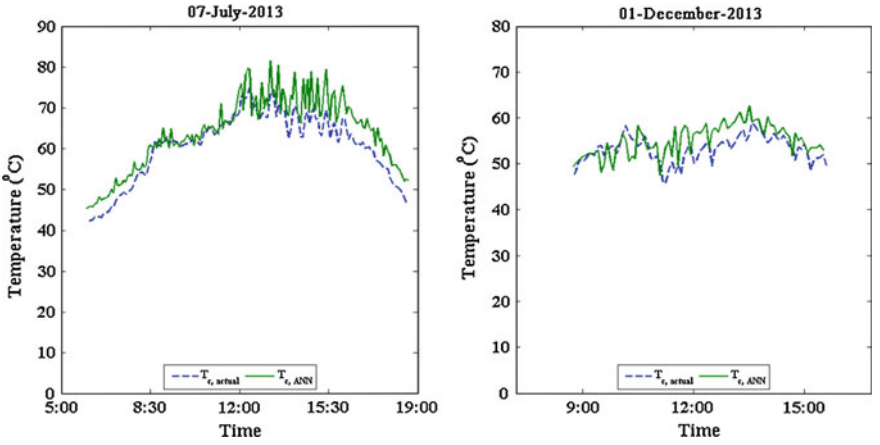

Fig. 4 *Left* Actual cell temperature versus predicted cell temperature by the ANN-based model for a summer day (07 July 2013). *Right* Actual cell temperature versus predicted cell temperature by ANN-based model for a winter day (01 December 2013)

Table 9 Values of the parameters R^2, RMSE, MAE, and MBE between actual and predicted data using Eqs. (6) and (7) for estimating the short-circuit current and the open-circuit voltage of the HCPV module considered

	R^2	RMSE (%)	MAE	MBE (%)
I_{sc}	0.97	3.53	0.12 A	−0.23
V_{oc}	0.90	0.66	0.29 V	0.01

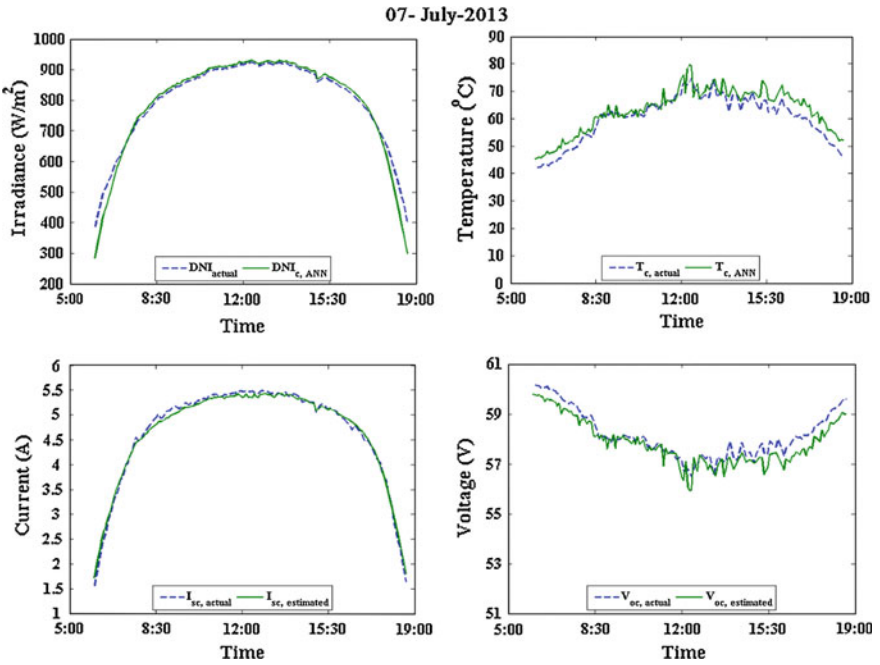

Fig. 5 *Top left* Direct normal irradiance measured during a summer day versus the spectrally corrected direct normal predicted by the ANN presented in [60]. *Top right* cell temperature measured during a summer day versus cell temperature predicted by the ANN presented in [41]. *Bottom left* Actual short-circuit current versus estimated short-circuit current using Eq. (6) for the HCPV module considered during a summer day. *Bottom right* Actual open-circuit voltage versus open-circuit voltage using Eq. (7) for the HCPV module considered during a summer day

Figures 5 and 6 bottom-left show the actual versus the predicted I_{sc} for the HCPV module considered for 2 example day. Figures 5 and 6 bottom-right show the actual versus the predicted V_{oc} for the HCPV module considered for 2 example days.

5 Conclusions

In this chapter, a review of ANN-based models developed for solving some problems related with HCPV technology is presented. In addition, several examples of the application of some of these models for estimating the main electrical parameters of an HCPV module—such as the P_m, the I_{sc}, and the V_{oc}—are presented.

The ANN based-model developed in [48] was applied to estimate the P_m of an HCPV. This model takes into account the main meteorological parameters that affect the output of an HCPV module. The approach presented in [58, 59] was

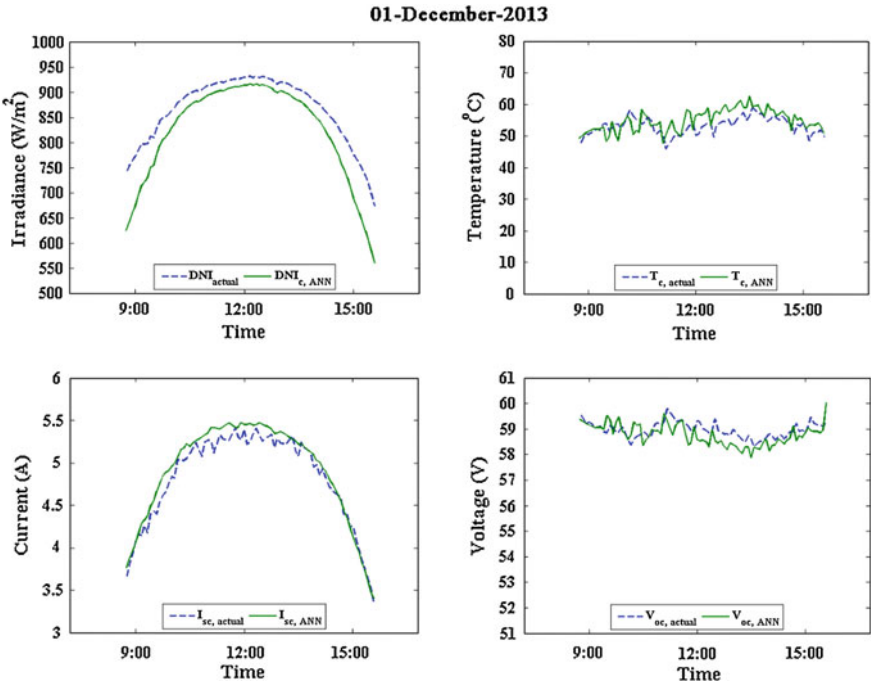

Fig. 6 *Top left* Direct normal irradiance measured during a winter day versus the direct normal predicted by the ANN presented in [60]. *Top right* cell temperature measured during a winter day versus cell temperature predicted by the ANN presented in [41]. *Bottom left* Actual short-circuit current versus estimated short-circuit current using Eq. (6) for the HCPV module considered during a winter day. *Bottom right* Actual open-circuit voltage versus open-circuit voltage using Eq. (7) for the HCPV module considered during a winter day

followed to estimate the I_{sc} and the V_{oc}. In this case, these electrical parameters were estimated from the DNI_c, the T_c, and use of the equations of conventional PVs. The values of the DNI_c and the T_c were obtained by applying the ANNs developed in [25, 60].

From the analysis of results, it can be concluded that ANNs are a useful tool for the electrical characterization of HPCV devices.

References

1. Luque A, Sala G, Luque-Heredia I (2006) Photovoltaic concentration at the onset of its commercial deployment. Prog Photovoltaics Res Appl 14(5):413–428
2. Xie W, Dai Y, Wang R, Sumathy K (2011) Concentrated solar energy applications using Fresnel lenses: a review. Renew Sustain Energy Rev 15(6):2588–2606
3. Pérez-Higueras P, Muñoz E, Almonacid G, Vidal P (2011) High concentrator photovoltaics efficiencies: present status and forecast. Renew Sustain Energy Rev 15(4):1810–1815

4. Dimroth F, Grave M, Beutel P et al (2014) Wafer bonded four-junction GaInP/GaAs/GaInAsP/GaInAs concentrator solar cells with 44.7 % efficiency. Prog Photovoltaics Res Appl 22(3):277–282
5. Ghosal K, Lilly D, Gabriel J, Whitehead M, Seel S, Fisher B, Wilson J, Burroughs S (2014) Semprius field results and progress in system development. IEEE J Photovoltaics 4(2): 703–708
6. Globaldata (2014) Concentrated photovoltaics (CPV)—global market size, competitive landscape and key country analysis to 2020. UK
7. Kalogirou S (2001) Application of artificial neural networks in renewable energy systems applications: a review. Renew Sustain Energy Rev 5:373–401
8. Mellit A, Kalogirou S (2008) Artificial intelligence techniques for photovoltaic applications: a review. Prog Energy Comb Sci 34:574–632
9. Kalogirou S (2000) Application of artificial neural networks for energy systems. Appl Energy 67:17–35
10. Hontoria L, Aguilera J, Riesco J, Zufiria P (2001) Recurrent neural supervised models for generating solar radiation. J Intell Rob Syst 31:201–221
11. Hontoria L, Aguilera J, Zufiria P (2002) Generation of hourly irradiation synthetic series using the neural network multilayer perceptron. Sol Energy 72(5):441–446
12. Al-Alawi S, Al-Hinai H (1998) An ANN-based approach for predicting global radiation in location with no direct measurement instrumentation. Renew Energy 14:199–204
13. Mellit A, Benghanem M, Hadj Arab A, Guessoum A (2005) A simplified model for generating sequences of global radiation data for insolates sites: using neural network and library of Markov transition matrices. Sol Energy 79(5):468–482
14. Mellit A, Benghanem M, Kalogirou S (2006) An adaptative wavelet-network model for forecasting daily total solar. Appl Energy 83:704–722
15. Bahgat A, Helwa N, Ahamd G, El Shenawy E (2004) Estimation of the maximum power and normal operating power of a photovoltaic module by neural networks. Renew Energy 29: 443–457
16. Himaya T, Katabayashi K (1997) Neural network based estimation of maximum power generation from PV module using environmental information. IEEE Trans Energy Convers 12 (3):241–247
17. Mellit A, Benghanem M, Hadj Arab A, Guessoum A (2005) An adaptive artificial neural network model for sizing stand-alone photovoltaic systems: application for isolated sites in Algeria. Renew Energy 30(10):1501–1524
18. Mellit A, Benghanem M, Kalogirou S (2007) Modelling and simulation of standalone photovoltaic system using an adaptative artificial neural network. Renew Energy 32(2): 285–313
19. Veerachary M, Yadaiah N (2000) ANN based peak power tracking for PV supplied motors. Sol Energy 69(4):343–350
20. Bahgat A, Helwa N, Ahamd G, El Shenawy E (2005) Maximum power point tracking controller for PV systems using neural networks. Renew Energy 30:1257–1268
21. Karapete E, Boztepe M, Colak M (2006) Neural network based solar cell model. Energy Convers Manag 47:1159–1178
22. de Blas M, Torres J, Prieto E, García A (2002) Selecting a suitable model for characterizing photovoltaic devices. Renew Energy 25:371–380
23. Almonacid F, Rus C, Hontoria L, Fuentes M, Nofuentes G (2009) Characterisation of Si-crystalline PV modules by artificial neural networks. Renew Energy 34:941–949
24. Almonacid F, Rus C, Hontoria L, Muñoz FJ (2010) Characterisation of PV CIS module by artificial neural networks. A comparative study with other methods. Renew Energy 35: 973–980
25. Almonacid F, Rus C, Pérez-Higueras P, Hontoria L (2011) Calculation of the energy provided by a PV generator. Comparative study: Conventional methods versus artificial neural networks. Energy 36:375–384

26. Almonacid F, Rus C, Pérez-Higueras P, Hontoria L (2009) Estimation of the energy of a PV generator using artificial neural network. Renew Energy 34:2743–2750
27. Coimbra CF, Kleissl J, Marquéz R (2013) Chapter 8: overview of solar-forecasting methods and a metric for accuracy evaluation. In: Solar energy forecasting and resource assessment, Elsevier, pp 172–192
28. Mellit A (2008) Artificial intelligence technique for modelling and forecasting of solar radiation data: a review. Int J Artif Intell Soft Comput 1(1):52–76
29. Lopez G, Batlles F, Tovar-Pescador J (2005) Selection of input parameters to model direct solar irradiance by using artificial neural networks. Energy 30:1675–1684
30. Alam S, Kaushik S, Garg S (2006) Computation of beam solar radiation at normal incidence using artificial neural network. Renew Energy 31:1483–1491
31. Mishra A, Kaushika N, Zhang G, Zhou J (2008) Artificial neural network model for the estimation of direct solar radiation in the Indian zone. Int J Sustain Energ 27(3):95–103
32. Mellit A, Eleuch H, Benghanem M, Elaoun C, Pavan A (2010) An adaptive model for predicting of global, direct and diffuse hourly solar irradiance. Energy Convers Manag 51:771–782
33. Mubiru J (2011) Using artificial neural networks to predict direct solar irradiation. Advan Artif Neural Syst 2011:1–6
34. Marquez R, Coimbra C (2011) Forecasting of global and direct solar irradiance using stochastic learning methods, ground experiments and the NWS database. Sol Energy 85: 746–756
35. Rodrigo J, Hontoria L, Almonacid F, Fernández E, Rodrigo P, Pérez-Higueras PJ (2012) Artificial neural networks for the generation of direct normal solar annual irradiance synthetic series. In: AIP conference proceedings of 8th international conference on concentrating photovoltaic systems: CPV-8, Toledo
36. Rehman S, Mohandes M (2012) Splitting global solar radiation into diffuse and direct normal fractions using artificial neural networks. Energy Sources 34(14):1326–1336
37. Marpu EYP, Gherboudj I, Ghedira H, Taha BO, Chiesa M (2013) Artificial neural network based model for retrieval of the direct normal, diffuse horizontal and global horizontal irradiances using SEVIRI images. Sol Energy 89:1–16
38. Chu Y, Pedro HT, Coimbra CF (2013) Hybrid intra-hour DNI forecasts with sky image processing enhanced by stochastic learning. Sol Energy 98:592–603
39. Fernández EF, Pérez-Higueras P, Garcia Loureiro A, Vidal P (2013) Outdoor evaluation of concentrator photovoltaic systems modules from different manufacturers: first results and steps. Prog Photovoltaics Res Appl 21(4):693–701
40. Fernandez EF, Almonacid F, Ruiz-Arias J, Soria-Moya A (2014) Analysis of the spectral variations on the performance of high concentrator photovoltaic modules operating under different real climate conditions. Sol Energy Mater Sol Cells 127:179–187
41. Fernández EF, Almonacid F, Rodrigo P, Pérez-Higueras P (2014) Calculation of the cell temperature of a high concentrator photovoltaic (HCPV) module: a study and comparison of different methods. Sol Energy Mater Sol Cells 121:144–151
42. Ef Fernández, Siefer G, Almonacid F, García Loureiro AJ, Pérez-Higueras P (2013) A two subcell equivalent solar cell model for III–V triple junction solar cells under spectrum and temperature variations. Sol Energy 92:221–229
43. Patra J, Maskell D (2010) Estimation of dual-junction solar cell characteristic using neural networks. In: 35th IEEE photovoltaic specialists conference, PVSC 2010, Honolulu
44. Patra J (2011) Neural network-based model for dual-junction solar cells. Prog Photovoltaics Res Appl 19:33–44
45. Patra J (2011) Chebyshev neural network-based model for dual-junction solar cells. IEEE Trans Energy Convers 26(1):132–139
46. Patra J, Maskell D (2012) Modeling of multi-junction solar cells for estimation of EQE under influence of charged particles using artificial neural networks. Renew Energy 44:7–16
47. "SILVACO," Available: http://www.silvaco.com/products/tcad/device_simulation/atlas/atlas.html

48. Almonacid F, Fernández EF, Rodrigo P, Pérez-Higueras P, Rus-Casas C (2013) Estimating the maximum power of a high concentrator photovoltaic (HCPV) module using an artificial neural network. Energy 53:165–172
49. Emery K, Del Cueto J, Zaaiman Z (2002) Spectral correction based on optical air mass. In: Proceeding of 29th IEEE PV specialist conference, New Orleans
50. Faine P, Kurtz SR, Riordan C, Olson J (1991) The influence of Spectral solar irradiance variations on the performance of selected single-junction and multijunction solar cells. Sol Cells 31:259–278
51. Kasten F, Young A (1989) Revised optical air mass tables and approximation formula. Appl Opt 28(22):4735–4738
52. Gueymard C (1992) Assesment of the accuracy and computing speed of simplified saturation vapour equations using a new reference dataset. J Appl Meteorol 32:294–300
53. Gueymard C (1994) Analysis of monthly average atmospheric precipitable water and turbidity in Canada and Northern United States. Sol Energy 53(1):57–71
54. Rigolliere C, Bauer O, Wald L (2000) On the clear sky model of the Esra—European Solar Radiation Atlas—with respect to the heliosat method. Sol Energy 68:33–38
55. Rivera A, García-Domingo B, Del Jesus M, Aguilera J (2013) Characterization of concentrating photovoltaic modules by cooperative competitive radial basis function networks. Expert Syst Appl 40(5):1599–1608
56. Williams S, Betts T, Helf T, Gottschalg R, Beyer H, Infield D (2003) Modeling long term module performance based on realistic reporting conditions with consideration to spectral effects. In: Proceedings of the world conference on photovoltaic energy conversion
57. Takashi M, Yasuhito N, Hiroaki T, Hideyuki T (2009) Uniqueness verification of solar spectrum index of average photon energy for evaluating outdoor performance of photovoltaic modules. Sol Energy 83:1294–1299
58. Antón I, Martinez M, Rubio F, Núñez R, Herrero R, Dominguez C, Victoria M, Askins S, Sala G (2012) Power rating of CPV systems based on spectrally corrected DNI. AIP Conf Proc 1477:331–335
59. King DL, Boyson WE, Kratochvil JA (2004) Sandia national laboratories. Photovoltaic array performance model SAND2004-3535, Albuquerque
60. Fernández E, Almonacid F (2014) Spectrally corrected direct normal irradiance based on artificial neural networks for high concentrator photovoltaic applications. Energy 74:941–949
61. Rodrigo P, Fernández E, Almonacid F, Pérez-Higueras P (2014) Review of methods for the calculation of cell temperature in high concentration photovoltaic modules for electrical characterization. Renew Sustain Energy Rev 38:478–488
62. Almonacid F, Pérez-Higueras P, Fernández EF, Rodrigo P (2012) Relation between the cell temperature of a HCPV module and atmospheric parameters. Sol Energy Mater Sol Cells 105:322–327
63. MODIS Daily Level-3 data (2013) Available: http://gdata1.sci.gsfc.nasa.gov/daac-bin/G3/gui.cgi?instance_id=MODIS_DAILY_L3. (Accessed 2013)